



Sharif University of Technology

**Scientia Iranica**

Transactions B: Mechanical Engineering

[www.sciencedirect.com](http://www.sciencedirect.com)

# Effect of 3D isotropic resolutions of sequenced images on natural vibration properties of trabecular bone

**Gokhan Altintas<sup>a,\*</sup>, Abdulkerim Ergut<sup>a</sup>, Ahmet Burak Goktepe<sup>b</sup>**

<sup>a</sup> Department of Civil Engineering, Faculty of Engineering, University of Celal Bayar, Muradiye Campus, Manisa, P.O. Box 45020, Turkey

<sup>b</sup> Fan River Hydropower Projects, Aydiner Const. Co., Lezha, Albania

Received 13 June 2012; revised 11 December 2012; accepted 21 January 2013

## KEYWORDS

Voxel;  
Finite element;  
Micro-ct;  
Natural vibration;  
Trabecular;  
Micro architecture.

**Abstract** The voxel based finite element (FE) method used to obtain primary data for non-invasive imaging techniques has emerged as a major focus of interest in several disciplines such as medicine, mechanics and material engineering for solving micro and nano-scale problems. Owing to the fact that, voxel based FE models are directly affected by parameters of imaging techniques such as Computed Tomography (CT) and Magnetic Resonance Imaging (MRI), the consequences of these effects on the natural vibration analysis of structures having complex geometry in micro scale, are investigated in this study. In this context, voxel based FE models are obtained using Micro-CT imaging data that has three different resolutions of vertebral trabecular bone tissue. Furthermore, resolutions of image data sets are artificially increased and equalized for evaluating voxel based FE models that are free from FE size effects. Natural vibration characteristics of voxel based FE models are investigated not only numerically but also including associated mode shapes. Unpredictable vibrational behavior for various voxel sizes, is, thus, revealed. Element size effects of voxel based FE models are considerably different from the effects on structural components with regular prismatic shapes. Obtained results show that, investigated parameters have a crucial influence on the natural vibration behavior of trabecular bone tissue which is selected as an example of complex geometries. Modal behaviors that are effective in micro local regions, but less in the whole body, where there are possibilities for working with approximate geometry without considering the micro structure have been observed. Moreover, the results are new from a theoretical point of view, and they also represent the importance of quality in imaging data, which, in practical applications must be taken into consideration.

© 2013 Sharif University of Technology. Production and hosting by Elsevier B.V.

Open access under [CC BY-NC-ND license](https://creativecommons.org/licenses/by-nc-nd/4.0/).

## 1. Introduction

CT and MRI imaging techniques are used for both imaging the internal structure of material and generating mechanical models with micro architectural detail. Owing to developments in CT and MRI technologies in recent years, meso-scale, and also micro and nano-scale geometries can be properly investigated. One of the most important results of these techniques is

providing information from structures in living tissue, which is impossible to perform using mechanical tests.

Within the content of this study, a literature review is compiled to underline the importance of the investigation, in which the formation of finite element modeling techniques and mechanical properties, as well as the behavior of bone structures, are examples of materials with complex geometries. Although surface and volumetric mesh generation techniques which are based on CT and MRI data, have been used for a long time, research on developing new algorithms and improved methods is continuously being undertaken to respond to many different types of problem of our day. In this context, Zhang et al. [1] built up a new algorithm to evaluate adaptive 3D meshes from volumetric image data, and have lately investigated an efficient approach to reconstruct unstructured tetrahedral and hexahedral meshes for mixed domains consisting of heterogeneous materials [2].

\* Corresponding author.

E-mail address: [gokhan.altintas@cbu.edu.tr](mailto:gokhan.altintas@cbu.edu.tr) (G. Altintas).

Peer review under responsibility of Sharif University of Technology.



Production and hosting by Elsevier

Finite element models working on high resolution sequenced imaging data enable micro-mechanical approaches, and the results of these models are accepted as a gold standard for the calibration of studies using classical continuum FE. Pahr and Zysset [3] examined the accuracy of a continuum FE model using Micro-FE as the gold standard. In this work, Micro-FE models were evaluated from high-resolution CT images. Eswaran et al. [4] revealed that Young's modulus and the density relation, particularly when assigned to the peripheral bone, substantially altered with regression coefficients, but not the degree of correlation between the continuum and Micro-FE predictions of whole-vertebral stiffness. Obviously, reconstruction procedures combined with FEM need rapid and strong software and hardware configurations. Soenke et al. [5] presented an extensive review of the reconstruction procedures. By the increasing number of the studies related to bone micro architecture, micro structural details gained significant importance in mechanical analysis. Lai et al. [6] have put forward regional differences in the trabecular bone of human cadavers using the values of bone mass density and details of the micro-architecture. Griffith and Genant [7] presented a notable study that although bone density has a significant effect on bone strength, it is not sufficient by itself and properties about micro architecture of bone should, especially be taken into consideration regarding bone strength. A study by Chevalier et al. [8] described that, voxel-based FE models of trabecular bone are combined with mechanical properties of volume fractions, Micro-CT reconstructions, mechanical tests, and sample specific nano indentation experiments for the validation method. In the study of N. Toosizadeh and M. Haghpahani [9], forces generated by muscles in different postures of the head were estimated. Furthermore, these muscle forces were also used to estimate internal cervical loads. Consequently, a geometrically accurate non-linear finite element model of C0–C7 was developed using CT images of the human cervical spine.

A three dimensional parametric model based on CT images of the lower cervical spine was investigated and validated by examining the model with some experimental data by Haghpahani and Javadi [10].

On the other hand, analysis results of the model may differ fundamentally due to the data and image processing techniques which have several calculation steps and optional variables. Particularly, resolutions of the slice thickness and parameters of segmentation of the images have an important effect on the reconstruction of voxel based FE models. Slice thickness and image resolution are both noteworthy parameters for simple images. The sensitivity of these parameters cannot be increased afterwards. In spite of the importance of this, a substantial part of the studies may be regarded as new. FE calculations of the apparent modulus were previously stated by Hara et al. [11] to be strongly affected by the threshold process applied for segmentation of CT data to construct the FE mesh. Furthermore, the moduli are substantially sensitive to error, due to the strong interaction between volume fraction and mechanical properties. In the study of Genant and Jiang [12], they compared the non-invasive imaging techniques with each other using trabecular bone tissue. The results are quite informative in terms of resolution values which are used during investigation of trabecular bone tissue. The relationship between CT slice intensity and the mechanical properties of porcine vertebral cancellous bone has also been investigated by Teo et al. [13].

Altintas [14] investigated the effect of slice thickness variation on the free vibration properties of Micro-CT based trabecular bone models. Bone structure is exposed to vibration in

Table 1: Quantitative properties of Micro-CT data set.

	Slice thickness and pixel edge length ( $\mu\text{m}$ )	Number of pixels on Micro-CT images	Number of slices
Micro-CT data set 1	36	$188 \times 188$	388
Micro-CT data set 2	72	$94 \times 94$	194
Micro-CT data set 3	144	$47 \times 47$	97

several cases and it has many steps containing vibration applications in diagnostics and treatment when microsurgery, micro injection, and osteoporosis treatment come into question. The natural vibration properties of bone structure were investigated in macro and micro scale by Cornelissen et al. [15], Altintas [14], and Altintas and Erdem [16] respectively. Cornelissen et al. [15] presented the influence of soft tissue on the stiffness of tibia. Perre and Lowet [17] studied sonic and ultrasonic wave propagation for the detection of osteoporosis. Perre and Lowet [17] used vibration and ultrasonic wave propagation analysis methods to determine the mechanical properties of bone.

Similar to the studies given above, there are also several contemporary studies available which involve vibration applications on determination of the mechanical properties of bones [18]. Medical vibration applications are very significant in current treatments as well [19,20].

Applications in micro-scale have been increased with developing technology. Vibration characteristics of structures in micro-scale may differ seriously from those in macro-scale. This difference especially comes from the fact that micro-architecture and parameters that take part in detecting micro-architecture methods must be used accurately.

For this purpose, in this study, it is aimed to investigate the effect of resolution values of imaging systems on the natural vibration behavior of micro structures. In addition, this study is directly performed according to isotropic voxel resolution unlike studies [14,16,21].

On the other hand, natural vibration properties were investigated not only by using voxel based FE methods evaluated from raw images with various resolutions but also using voxels that derived from images with artificially increased resolutions which are free from FE size effects in this study. Since many medical applications and reconstruction programs are modeled according to isotropic voxels, this study is considered valuable in theoretical, and also in practical applications.

## 2. Material and method

Three different Micro-CT data sets as given in Table 1 belonging to the same lumbar vertebral body (L3) sample and also having 36, 72 and 144  $\mu\text{m}$  pixel side lengths and slice interval values are used. Region of Interest (ROI) as seen in Figure 1 is selected as trabecular bone structure tissue from an original Micro-CT data set which has 45.806 mm<sup>2</sup> square cross section area, side length and 13.968 mm extent. Each slice in the Micro-CT data set is in TIFF format and grayscale values of pixels in image files were linearly scaled to cover the range from 0 to 255 for minimal and maximal values, correspondingly.

### 2.1. Methodology of the conversion process of sequenced images to finite element model

In this investigation, frequency values in natural vibration modes and mode shapes are obtained using the ABAQUS® FE

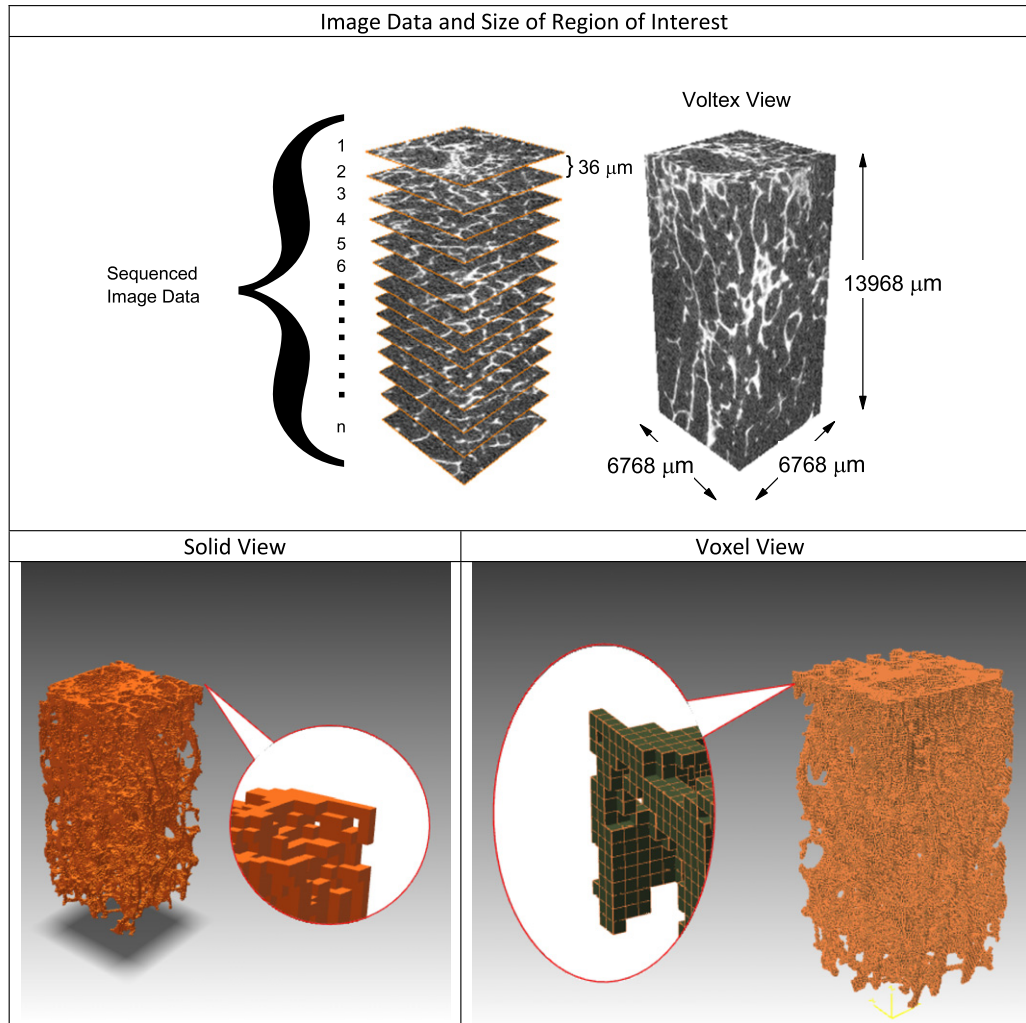


Figure 1: Trabecular bone structure (Region of Interest).

analysis program. It is possible to convert sequenced image files in Micro-CT data sets into one finite element model which is analyzed by ABAQUS® by applying several imaging and morphologic processes consecutively.

For this purpose, a MATLAB® script named CUBOID-SI2FE is developed by Altintas [14] and Altintas and Erdem [16]. CUBOID-SI2FE is a compact software containing threshold, reconstruction, and a specific flood fill algorithm [22] in itself, which makes it possible to convert sequenced image files to FE input ones which are solvable by the ABAQUS® program directly. The below mentioned processes are completely carried out within CUBOID-SI2FE. Imaging data in Micro-CT data set are formed as three dimensional brick shaped voxel elements by adding slice thickness to pixels. During this process, the number of voxel elements and nodes are properly given according to the ABAQUS® input file, and grayscale values of pixels are assigned into related voxels. As the square pixel edge length and pixel distance are known, each pixel can be alleged to form the basis of cubic shaped voxels with a height equal to the slice to slice distance. Threshold range determined by visual confirmation is used in deciding which voxels belong to bone tissue, and they are separated from other tissue in this way. In this step, converting voxel elements marked as bone tissue into the ABAQUS® input file is done with CUBOID-SI2FE by defining the linear hexahedral elements of type C3D8 and reorganizing

elements and nodes. The C3D8 element is a general purpose eight node linear brick element, fully integrated ( $2 \times 2 \times 2$  integration points). Due to the full integration applied for deriving of C3D8, the element is suitable for non-isochoric material.

Although converting to the FE model according to analysis of serial imaging data by ABAQUS® in the above explained process seems probable, it is not possible to perform analyses without adding some procedures in many cases. Due to the fact that the discrete voxels derived by the threshold procedure do not guarantee interconnected bone tissue whose models have discontinuity, it is not possible to perform eigenvalue analyses as natural frequency or buckling. For providing continuity, a fast and efficient flood fill algorithm was developed in a different way from well-established flood fill and region growing algorithms. The flood fill algorithm was established into CUBOID-SI2FE for processing files in the form of an ABAQUS® input file data structure.

## 2.2. Node-ID based Flood fill algorithm

Voxelization and solidification processes are not adequate for reconstruction of models that can be used for the solution of mechanical problems. Three dimensional Flood fill

algorithms must be used particularly for mechanical calculations including natural frequency and buckling type eigenvalue analyses. Flood fill algorithms remove some structures such as undesired and unconnected parts, islands etc., which do not actually exist in the model. The flood fill algorithm is an inseparable part of much commercial software such as Mimics® (Materialise®), which creates input files for mechanical analysis programs. There are many current studies suggesting new versions of the flood fill algorithm [19] and similar algorithms, for analyses [23–26]. The algorithm presented in this study is prepared for the requirement of processing input files of ABAQUS®. For providing continuity and removing islands, the CUBOID-SI2FE script is redesigned to apply the flood fill algorithm to data structures derived directly from Micro-CT data sets or ABAQUS® input files.

Some definitions shall be stated to explain the algorithm. In the flood fill algorithm,  $V_{UW}$  is a domain made up of  $V_i$  unit cubic elements.

$$V_{UW} = \sum_{i=1}^N V_i. \quad (1)$$

Each  $V_i$  cubic element can be expressed as follows, according to the number of cubic elements and nodes:

$$V_i \rightarrow [E_i, p_i \cdots p_s]. \quad (2)$$

$E_i$  is the cubic number of voxel element  $V_i$ . Side points are stated by  $p_i$  and  $s$  subscript shows the total point numbers of the voxel element. The coordinate calculation of the elements is not necessary for application in the algorithm. Points of the cubic element are enough for the solution. If any two elements have a cluster of common points with a size equal to the number of points on one surface of the voxel element, these elements are considered neighbors and have a matched surface.

To confirm this conclusion precisely;

- Volumetric voxel elements must have convex geometry.
- Surfaces of the volumetric voxel element must be planar.
- Sides of planar surfaces must be in a straight line form.

### 3. Analysis and results

The effects of the resolution of Micro-CT images of trabecular bone structure and the influence of slice thickness, on the natural vibration behavior of voxel based FE models, are fundamentally targeted and investigated. Within this scope, it is determined that the zone accepted as bone tissue in grayscale corresponds to the 135–255 range. Threshold segmentation is also applied by CUBOID-SI2FE to Micro-CT imaging data for these values, and finally, imaging data is prepared for a three dimensional reconstruction process. The models are obtained with two different approaches to present the effect of resolution on natural vibration. The first of these is reconstructing the voxel based models by means of the original resolutions of Micro-CT data. In the second approach, element sizes of all models are equalized by increasing resolutions of all image data sets artificially.

Although image resolutions were increased, micro structural details were not really increased as seen in Figure 2. By this means, it is aimed to procure the results free from the finite element size effect. One part of the sample geometry, shown in Figure 2(a), is obtained for various resolutions and approaches. Detailed images are presented to make the comparison of the models more comprehensive. Voxel based models using the original resolution of Micro-CT data are given in Figure 2(b),

(c) and (e). The models in Figure 2(d) and (e) are obtained from the models seen in Figure 2(c) and (e), correspondingly, by reducing the element sizes to 36  $\mu\text{m}$  which is equal to the highest resolution of all image data sets. Because models with 72  $\mu\text{m}$  and 144  $\mu\text{m}$  edge size have their high resolution pairs, it is possible to perform analyses and make comparisons free from FE size effects.

Basic geometric properties and FE mesh properties of evaluated models are given in Table 2. Volumes of the voxel based models (Models 1, 2, 4) with original resolutions increase by incrementation of the resolutions. On the other hand, increments in surface area for resolution have occurred much larger than the volumetric increment. This inference is important in terms of medical applications, and presents the significance of surface area related problems, such as porous fluid flow [27,28] or medical applications [29–31] by dealing in details without any loss due to working at high resolution. In another perspective, the complexity of the object geometry may improve when the volume remains almost constant and surface area increases.

It is almost impossible to present a meaningful relationship, including all modes for different models, when only the frequency values of the modes in Table 3 are investigated. When the alteration probability of morphological differences on natural vibration behavior among models as anisotropic voxel sizes, is used, as in the study of Altintas [14], Altintas and Erdem [16], evaluation of free vibration modes with mode shapes as well as frequency values would enable better interpretation of the results. Modal behavior of the systems is investigated by checking the mode shapes that are partly given in Figure 3 due to distinctive forms of zones where maximum displacements occur. In this paper, mode shapes in Figure 3 shall be investigated in the first place before evaluating the modal behavior of the investigated systems. The zones where maximum displacements take place, belonging to the fundamental mode shapes of voxel based FE models for various image set resolutions, are presented in the first line of Figure 3. Frequency values of fundamental modes are 6401.9, 6001.5 and 6413.3 Hz for models that have 36, 72 and 144  $\mu\text{m}$  pixel side lengths, respectively. While mode structures of the first two models correspond to each other, the part where maximum displacements occur in the model having 144  $\mu\text{m}$  pixel side lengths is considerably different from both the morphologic structure and the connected zone. It can be stated according to the mode shapes in the first line of Figure 3 that mode shapes of models obtained from images having various resolution values may be different, even if they are all in fundamental mode. While the mode shapes in the second line of Figure 3 are almost the same for each of the 3 models, there are differences observed in mode number and natural frequency values in the related systems. The fifth mode of the model obtained from scanning images that have the highest resolution value, with 36  $\mu\text{m}$  pixel width, corresponds to the 6th mode of the model derived from the images having 72  $\mu\text{m}$  pixel width and whose voxel edge sizes are reduced from 72 to 36  $\mu\text{m}$ . Those modes occur in 13253.4, 9189.1, 9655 Hz frequency values, respectively. The third line of Figure 3 can be examined to observe the different mode order of the example which can also be defined as the same mode. The order of the modes whose model evaluated from the data set original resolution has 36 and 76  $\mu\text{m}$  pixel edge lengths, is the same as the 6th and 12th modes. The subjected mode occurs in the 11th order of the model whose pixel edge length is artificially reduced from 72  $\mu\text{m}$  to 36  $\mu\text{m}$ .



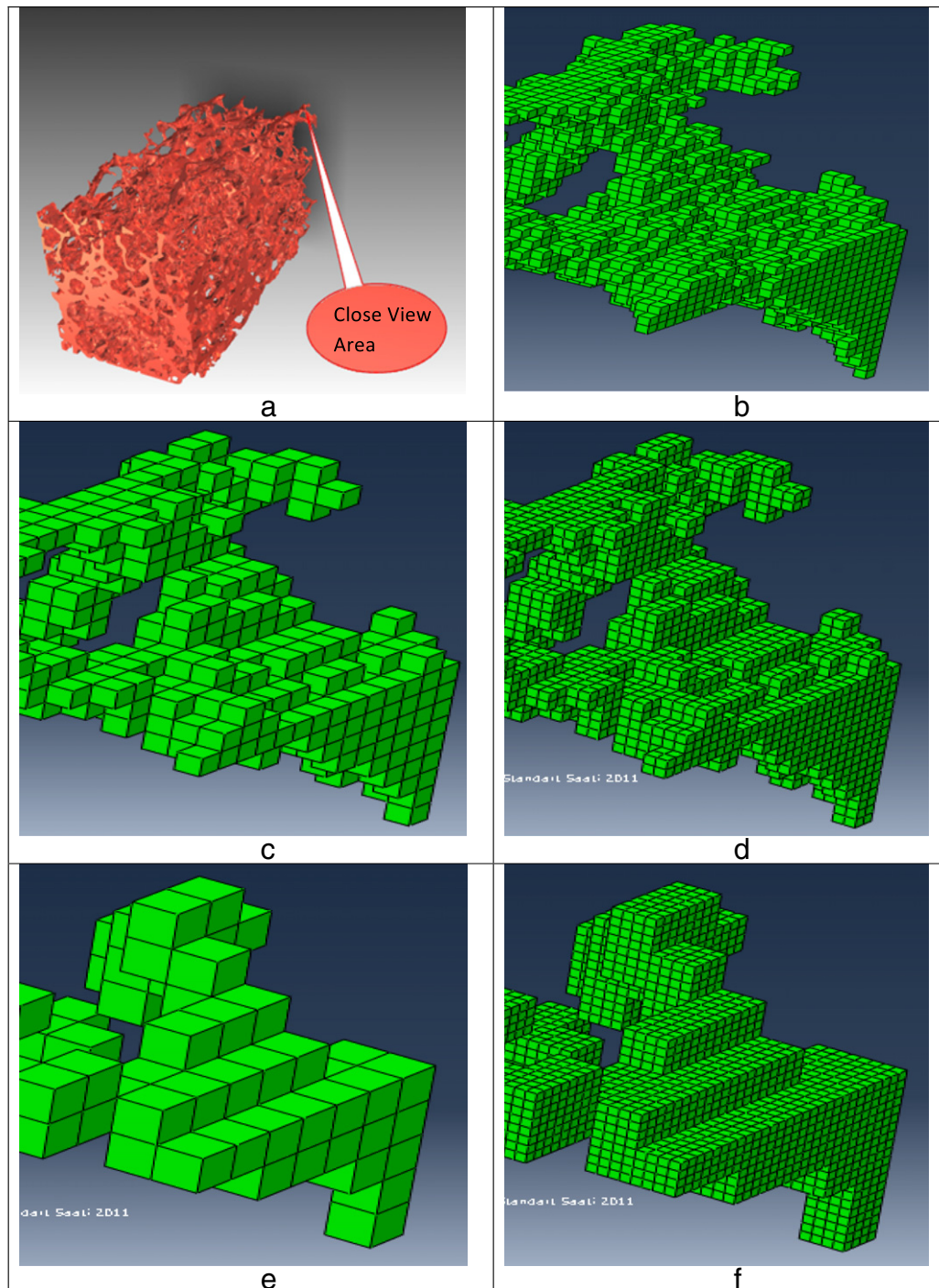


Figure 2: Close views of the models: (a) ROI and signed close view area; (b) Voxel based model with  $36\ \mu\text{m}$  edge size (Original Resolution, Model 1); (c) Voxel based model with  $72\ \mu\text{m}$  edge size (Original Resolution, Model 2); (d) Model with artificially reduced element edge size  $72\text{--}36\ \mu\text{m}$  (Model 3); (e) Voxel based model with  $144\ \mu\text{m}$  edge size (Original Resolution, Model 4); (f) Model with artificially reduced element edge size  $144\text{--}36\ \mu\text{m}$  (Model 5).

The general evaluations given below are approached by considering both mode shape and natural frequencies in Figure 3 together in order to understand the modal behaviors of the investigated systems more easily. When the natural vibration behavior of voxel based models that have different resolutions are compared with each other, the frequency values of mode structures that are accepted as the same mode increase according to resolution increment. It is impossible to state this situation as a rule. Although there are many modes

corresponding to this rule in the investigated mode range, there are also a few which are not in accordance with the rule.

Mode shape, frequency, and order of models are affected by image resolutions directly. The mode shape appearing in one model could occur in a different queue in another mode, or not even appear at all. On the other hand, voxel based finite elements models that have  $144\ \mu\text{m}$  side lengths and are obtained from images having the lowest resolution, have such different modal behavior that cannot be compared with mode

Table 2: Primary shape and finite element properties of models.

Model number	Models				
	(1)	(2)	(3)	(4)	(5)
Model description	Voxel based model with 36 $\mu\text{m}$ edge size	Voxel based model with 72 $\mu\text{m}$ edge size	Model with artificially reduced element edge size 72–36 $\mu\text{m}$	Voxel based model with 144 $\mu\text{m}$ edge size	Model with artificially reduced element edge size 144–36 $\mu\text{m}$
Volume $\text{mm}^3$	88.617	87.567	87.567	86.674	86.674
Surface area $\text{mm}^2$	2552.202	2181.759	2181.759	1574.004	1574.004
Number of nodes	2 930 333	459 500	2 749 651	72 033	2 488 242
Number of elements	1 899 363	234 608	1 876 864	29 027	1 857 728

Table 3: First twenty natural frequencies of models (Hz).

Model number	(1)	(2)	(3)	(4)	(5)
Model description	Voxel based model with 36 $\mu\text{m}$ edge size	Voxel based model with 72 $\mu\text{m}$ edge size	Model with artificially reduced element edge size 72–36 $\mu\text{m}$	Voxel based model with 144 $\mu\text{m}$ edge size	Model with artificially reduced element edge size 144–36 $\mu\text{m}$
1	6401.9	6001.5	5699.7	6770.1	6413.3
2	9097.6	7065.5	6693.9	8372.7	7512
3	10 178.1	7669.4	7525.2	8636.8	7987
4	10 245	8586	8850.5	10 570.6	9859
5	13 253.4	8895.4	8972.2	10 654	9917.3
6	14 575	9189.1	9655	10 962.8	10 346.4
7	15 509.2	10 416.3	10 415.4	12 084.5	10 770.2
8	16 564.1	12 420.6	11 480.1	13 111.8	11 558.9
9	20 484.3	12 949.2	12 264.7	13 492.5	12 112.1
10	22 406.7	15 653.5	14 771.9	13 554.8	12 197.2
11	22 885.9	17 955.7	17 253.4	14 557.8	13 296.6
12	23 236	18 949.3	17 584.6	15 339.3	14 248.4
13	23 376.6	19 271.6	17 733.6	16 013.6	14 379.9
14	25 747.4	20 590.5	18 786	16 203.6	14 543.5
15	26 004	22 143.2	20 453.7	16 510.2	14 741.1
16	26 259.4	22 859.6	21 099.2	17 084.1	15 315.7
17	26 446.4	22 925.9	21 633.6	18 756.4	16 742
18	27 585.6	23 178.4	22 354.4	19 501.1	17 508.5
19	28 565.9	23 332	23 270.8	19 834.5	17 800.8
20	29 619.3	26 340.4	24 858.5	20 335.7	18 931

shapes obtained from the models having 36 and 72  $\mu\text{m}$  side length. The most significant reason for this situation is the fact that realistic modeling can be made by current resolutions each material having its own. Resolution values about 60  $\mu\text{m}$  are generally accepted as the limit for trabecular bone tissue in vertebrae without losing any detail [12]. For this reason, while the mode shapes of voxel based FE models having 36  $\mu\text{m}$  and 72  $\mu\text{m}$  side lengths can be compared with each other, the range of modes, according to the model with 144  $\mu\text{m}$  side length is numerically quite different from the others. This situation shows the importance of evaluating mode shape and numerical value together. The frequency range at which modes appear in the same numbers becomes narrow, according to the resolution increment for voxel based FE models.

In this investigation, some parts of the investigated systems are designed to analyze results free from finite element size effects, and general comments are made for investigations within this scope. By comparing the models whose original voxel side lengths are 144 and 72  $\mu\text{m}$  and the models whose element side lengths are reduced to 36  $\mu\text{m}$  and derivations of these models having the same geometric boundaries and volumes, there are some outcomes appeared, which are hard to estimate due to FE size effects, and usually encountered in objects that are geometrically prismatic shaped. One of the

most important points of this situation is that, although having natural frequency values regarding the natural vibration modes of models whose sizes are reduced and which usually result in lower values as expected, there are still some modes against this rule.

To give an example, the first three natural vibration modes of the model whose original voxel side length is 72  $\mu\text{m}$  are bigger than the derived model which has 36  $\mu\text{m}$  side length as expected. However, the situation changes quite the opposite for the next 3 modes. This situation depending on the element size of these modes, which are approved as the same, according to mode shape is not frequently encountered in prismatic objects.

Models which have the same surface and volumetric properties but different element sizes differ from mode structures at the same time, and this difference changes the mode orders as well as gives rise to different constituted modes from another. If it is necessary to give an example of this situation, it can be stated that even though modes in Figure 3(h) and (i) are the same, they have different mode numbers because the appearance of a mode in the model does not show up in another.

The close view sections of shapes where maximum displacement occurs are taken into consideration in comparison.

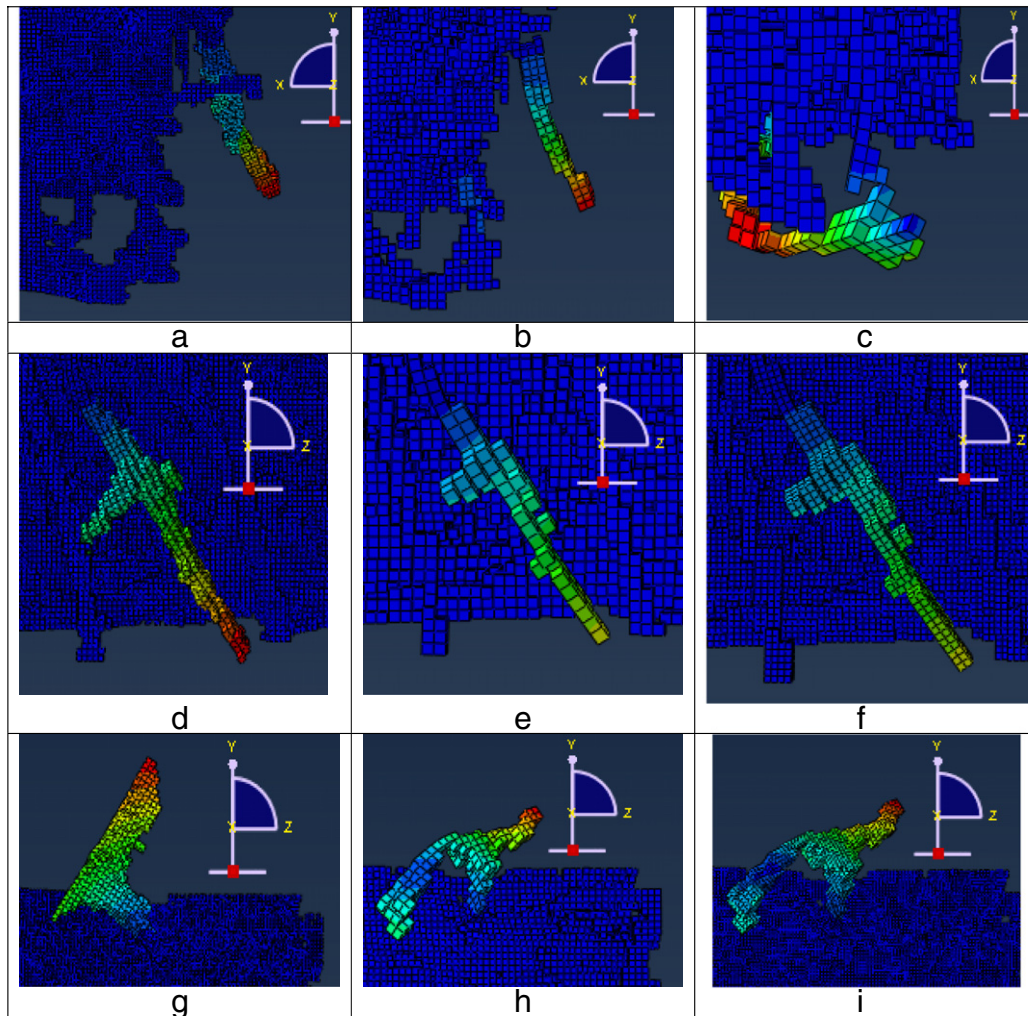


Figure 3: Comparison of the modes for maximum displacement fields of mode shapes (a) Voxel based model with 36  $\mu\text{m}$  edge size FUNDAMENTAL MODE (Model 1); (b) Voxel based model with 72  $\mu\text{m}$  edge size FUNDAMENTAL MODE (Model 2); (c) Voxel based model with 144  $\mu\text{m}$  edge size FUNDAMENTAL MODE (Model 3); (d) Voxel based model with 36  $\mu\text{m}$  edge size 5.MODE (Model 1); (e) Voxel based model with 72  $\mu\text{m}$  edge 6.MODE (Model 2); (f) Model with artificially reduced element edge size 72–36  $\mu\text{m}$  6.MODE (Model 3); (g) Voxel based model with 36  $\mu\text{m}$  edge size 6.MODE (Model 1); (h) Voxel based model with 72  $\mu\text{m}$  edge 12.MODE (Model 2); (i) Model with artificially reduced element edge size 72–36  $\mu\text{m}$  11.MODE (Model 3).

It should be underlined that the models obtained from various images with different resolutions are not precisely the same objects.

#### 4. Conclusions

The effect of three dimensional isotropic resolutions of sequenced images on the modal behavior of trabecular bone is a good example of a complex geometrical structure. In this study, voxel based FE models are derived from two type image data sets, some of which have original resolutions and where others have artificially increased resolutions for preventing FE size effects. Due to different resolutions of image data sets, additional or missing connections of models that change system stiffness may affect natural frequency behavior. However, it is observed that, connection differences cause distinctive variances on mode shape, as well as numerical values of natural frequencies. There have been remarkable changes not only in the values of natural vibration modes according to resolution change, but also on mode shapes. While the mode appears in one model, it does not appear in another, or it can be seen in

another mode order for models which occur in models having different resolution values from each other. It is impossible to explain this with a certain rule, depending on resolution according to frequency values at which mode structures that are almost same as each other appear. The frequency range for the first 20 modes increases in parallel for increments of resolution values without considering mode type. This situation does not change for models that are not affected by derivation or free from FE size effects.

Generally, it is seen that complex geometry such as trabecular bone tissue has been significantly affected by the quality of imaging data. Parts of the investigated modes appear as very small regions which are primarily caused by large displacements of natural frequencies in a micro scaled study. This situation is a crucial detail that cannot be obtained from the solution of a single prismatic system in which geometry is approximately taken into account.

The obtained results are important in theory and it is also believed that they will be helpful while evaluating practical cases due to voxel based FE model applications.

## References

- [1] Zhang, Y., Bajaj, C. and Sohn, B. "3D finite element meshing from imaging data", *Computational Methods in Applied Mathematics*, 194, pp. 5083–5106 (2005).
- [2] Zhang, Y., Hughes, T.J.R. and Bajaj, C.L. "An automatic 3D mesh generation method for domains with multiple materials", *Computational Methods in Applied Mathematics*, 199, pp. 405–415 (2010).
- [3] Pahr, D.H. and Zysset, P.K. "A comparison of enhanced continuum FE with micro FE models of human vertebral bodies", *Journal of Biomechanics*, 42, pp. 455–462 (2009).
- [4] Eswaran, K.S., Fields, A.J., Nagarathnam, P. and Keaven, T.M. "Multi-scale modeling of the human vertebral body: comparison of Micro-CT based high resolution and continuum-level models", *Pacific Symposium on Biocomputing*, 14, pp. 293–303 (2009).
- [5] Soenke, H.B., Wolfram, S., Wolfhard, S. and Fabian, K. "Small animal computed tomography imaging", *Current Medical Imaging Reviews*, 3, pp. 45–59 (2007).
- [6] Lai, Y.M., Quinb, H.Y., Lee, K.K.H. and Chan, K.M. "Regional differences in trabecular BMD and micro-architecture of weight-bearing bone under habitual gait loading—A pQCT and Micro-CT study in human cadavers", *Bone*, 37, pp. 274–282 (2005).
- [7] Griffith, J.F. and Genant, H.K. "Bone mass and architecture determination: state of the art", *Journal of Clinical Endocrinology & Metabolism*, 22(5), pp. 737–764 (2008).
- [8] Chevalier, Y., Pahr, D., Allmer, H., Charlebois, M. and Zysset, P. "Validation of a voxel-based FE Method for prediction of the uniaxial apparent modulus of human trabecular bone using macroscopic mechanical tests and nanoindentation", *Journal of Biomechanics*, 40, pp. 3333–3340 (2007).
- [9] Toosizadeh, N. and Haghpahani, M. "Generating a finite element model of the cervical spine: estimating muscle forces and internal loads", *Scientia Iranica*, 18(6), pp. 1237–1245 (2011).
- [10] Haghpahani, M. and Javadi, M. "A three dimensional parametric model of whole lower cervical spine (C3–C7) under flexion, extension, torsion and lateral bending", *Scientia Iranica*, 19(1), pp. 142–150 (2012).
- [11] Hara, T., Tanck, E., Homminga, J. and Huiskes, R. "The influence of micro-computed tomography threshold variations on the assessment of structural and mechanical trabecular bone properties", *Bone*, 31, pp. 107–109 (2002).
- [12] Genant, H.K. and Jiang, Y. "Advanced imaging assessment of bone quality", *Annals of the New York Academy of Sciences*, 1068, pp. 410–428 (2006).
- [13] Teo, J.C.M., Si-Hoe, K.M., Keh, J.E.L. and Teoh, S.H. "Relationship between CT intensity, micro-architecture and mechanical properties of porcine vertebral cancellous bone", *Clinical Biomechanics*, 21, pp. 235–244 (2006).
- [14] Altintas, G. "Effect of slice thickness variation on free vibration properties of Micro-CT based trabecular bone models", *2nd International Symposium on Computing in Science & Engineering*, Kuşadası, TURKEY (June 1–4, 2011).
- [15] Cornelissen, M., Cornelissen, P., Perre, G., Christensen, A., B., Ammitzbohl, F. and Dyrbye, C. "Assessment of tibial stiffness by vibration testing in situ-III. Identification of mode shapes in different supporting conditions", *Journal of Biomechanics*, 20, pp. 333–342 (1986).
- [16] Altintas, G. and Erdem, R.T. "Effect of Micro-CT slice intensity on natural vibration behavior of cancellous bone models based on reverse engineering techniques", *Procedia Technology*, 1, pp. 318–322 (2012).
- [17] Perre, G. and Lowet, G. "Vibration, sonic and ultrasonic wave propagation analysis for the detection of osteoporosis", *Clinical Rheumatology*, 13, pp. 45–53 (1994).
- [18] Bediz, B., Özgüven, H.N. and Korkusuz, F. "Vibration measurements predict the mechanical properties of human tibia", *Clinical Biomechanics*, 25, pp. 365–371 (2010).
- [19] Wenger, K.H., Freeman, J.D., Fulzele, S., Immel, D.M., Powell, B.D., Molitor, P., Chao, Y.J., Gao, H.S., Elsalanty, M., Hamrick, M.W., Isaacs, C.M. and Yu, J.C. "Effect of whole-body vibration on bone properties in ageing mice", *Bone*, 47(4), pp. 746–755 (2010).
- [20] Shih, F.Y. and Cheng, S. "Automatic seeded region growing for color image segmentation", *Image and Vision Computing*, 23(10), pp. 877–886 (2005).
- [21] Altintas, G. "Effect of slice step size on prediction of natural vibration properties of bone tissue", *Mathematical and Computational Applications*, 17(3), pp. 235–243 (2012).
- [22] Altintas, G. "Node-id based non-recursive flood fill algorithm for non-uniform discrete solid domains", *2nd World Conference On Information Technology*, Antalya, Turkey, November 23–27 (2011).
- [23] Lu, Y., Miao, J., Duan, L., Qiao, Y. and Jia, R. "A new approach to image segmentation based on simplified region growing PCNN", *Applied Mathematics and Computation*, 205, pp. 807–814 (2008).
- [24] Malek, A.A., Rahman, W.E.Z.W.A., Ibrahim, A., Mahmud, R., Yasiran, S.S.A. and Jumaat, K. "Region and boundary segmentation of micro calcifications using seed-based region growing and mathematical morphology", *Procedia Social and Behavioral Sciences*, 8, pp. 634–639 (2010).
- [25] Wu, Y., Li, M., Zhang, P., Zong, H., Xiao, P. and Liu, C. "Unsupervised multi-class segmentation of SAR images using triplet Markov fields models based on edge penalty", *Pattern Recognition Letters*, 32(11), pp. 1532–1540 (2011).
- [26] Guoying, Z., Hong, Z. and Ning, X. "Flotation bubble image segmentation based on seed region boundary growing", *Mining Science and Technology*, 21(2), pp. 239–242 (2011).
- [27] Nadeem, S., Akbar, N.S. and Malik, M.Y. "Numerical solutions of peristaltic flow of a Newtonian fluid under the effects of magnetic field and heat transfer in a porous concentric tubes", *Zeitschrift für Naturforschung*, 65(a), pp. 369–380 (2010).
- [28] Nadeem, S., Akbar, N.S. and Malik, M.Y. "Exact and numerical solutions of a micropolar fluid in a vertical annulus", *Numerical Methods for Partial Differential Equations*, 26(6), pp. 1660–1674 (2010).
- [29] Nadeem, S. and Akbar, N.S. "Exact and numerical simulation of peristaltic flow of a non-Newtonian fluid with inclined magnetic field in an endoscope", *International Journal for Numerical Methods in Fluids*, 66(7), pp. 919–934 (2011).
- [30] Nadeem, S. and Akbar, N.S. "Numerical solutions of peristaltic flow of Williamson fluid with radially varying MHD in an endoscope", *International Journal for Numerical Methods in Fluids*, 66(2), pp. 212–220 (2011).
- [31] Nadeem, S. and Akbar, N.S. "Numerical analysis of peristaltic transport of a tangent hyperbolic fluid in an endoscope", *Journal of Aerospace Engineering*, 24(3), pp. 309–317 (2011).

**Gokhan Altintas** received his BS degree in Civil Engineering from Dokuz Eylul University, Turkey, in 1992, his MS degree from Celal Bayar University, Turkey, in 1996, where he is currently working as Associate Professor, and his Ph.D. degree in Vibration Mechanics in Civil Engineering from Yildiz Technical University, Turkey, in 2002. His research interests include: modal analysis, voxel based finite element methods, computer simulations, and reverse engineering problems.

**Abdulkemir Ergut** received his BS degree in Civil Engineering from Osmangazi University, Turkey, in 2004, and his MS degree from Celal Bayar University, Turkey, in 2008, where he is currently working as research assistant and studying for his Ph.D. degree in Civil Engineering. His research interests include: vibration of plates, FEM, reverse engineering and image processing.

**Ahmet Burak Goktepe** was born in Turkey, in 1970. He obtained his BS, MS, and Ph.D. degrees from Istanbul Technical University, Turkey, and has worked in universities and the private sector for many years. His research interests include: geotechnical engineering, material science, FEM, simulation, numerical modelling, statistical analyses and soft computing.